^{63}Cu^{q+} and ^{197}Au^{q+} ion beam induced sputtering of ITO coated glass thin films at 0.1 MeV/u – 0.6 MeV/u SIMS energies

G T Mafa[1,2]**, T P Sechogela**[1] **and M Msimanga**[1,2]

[1] Department of Physics, Tshwane University of Technology, Private Bag X680, Pretoria, 0001, South Africa

[2] iThemba LABS TAMS, National Research Foundation, Private Bag 11, WITS, 2050, Johannesburg, South Africa

Email: Granttshepo02@gmail.com

Abstract. Ion beam induced sputtering in matter is of interest for fundamental ion-atom interaction studies. It is also important for practical applications such as ion beam materials analysis techniques like Secondary Ion Mass Spectrometry at MeV ion energies (MeV SIMS). Theoretical descriptions of nuclear sputtering yields due to keV projectile ions are generally in good agreement with experimental data, but this is not the case for electronic sputtering yields using heavy projectile ions There is thus a need for experimental data to improve existing theoretical models that describe electronic sputtering due to MeV ions. This work presents results of thin film sputtering yield measurements carried out using the Elastic Recoil Detection Analysis technique (ERDA). Measurements were carried out to determine the electronic sputtering yield in Indium Tin Oxide (ITO) due to ^{63}Cu^{q+} and ^{197}Au^{q+} MeV ion beams over an ion velocity range of 0.1 MeV/u - 0.6 MeV/u. The UV-Vis characterization technique was also used to determine the changes in the optical properties of the conducting oxide films due to heavy ion beam irradiation. Results show that reduction in thickness of the ITO film is attributed to the preferential sputtering of oxygen from the surface. The measured sputtering yield data were found to decrease with increasing ion fluence in the ITO target material for both Au and Cu ion beams. The optical band gap was found to decrease only slightly from 3.99 eV (for pristine) to 3.93 eV with increasing ion fluence. The results, in general, indicate that heavy ion beams irradiation can be used as an effective tool to induce surface modifications in thin films by dense electronic excitation.

1. Introduction

The sputtering of atoms from a solid thin film by heavy ion beam bombardment is of practical interest in areas related to materials analysis and modification, and for understanding the fundamentals of heavy ion interaction with matter.

Sputtering of ions in matter has been studied extensively over the years [1,2]. Although a lot of research on sputtering yields induced by ion-target nuclei collisions at keV energies has been done in this field, this has not been the case for sputtering yields induced by interactions between high energy (MeV) projectile ions and orbital electrons of target atoms. Nuclear sputtering yields at keV energies can be predicted fairly accurately by existing sputtering theories [3] for practical applications in the traditional keV SIMS technique for instance. SIMS is a mass spectrometry technique that involves

bombarding the surface of a sample with a beam of accelerated ions and analyzing the secondary ions produced by the ion bombardment [4]. The predictive accuracy of existing models for electronic sputtering due to MeV ions is still inadequate for many practical applications, thus more experimental data is needed for the improvement and validation of theory. In this work we present experimental sputtering yield results in thin films due to heavy ion beam bombardment in the context of possible applications in MeV SIMS.

Sputtering occurs when a solid target sample is subjected to irradiation with energetic ions resulting in particles being ejected from the surface. The projectile particle loses energy to the target via two mechanisms, which are central aspects in the theory of ion-matter interaction: inelastic electronic losses (ionization, electron-electron collisions, electronic excitation, and charge transfer) and elastic nuclear collisions (atom-atom collisions and conserved kinetic energy) [3]. The energy of the incident ions determines which energy loss will be dominant. At low projectile energies (< 100 keV/nucleon) the dominant mode of ion-target interaction is through nuclear collision cascades, which lead to nuclear sputtering. As the projectile energy increases, its energy loss tends to be mostly due to interaction with the electron cloud of the target atom than with the nucleus, this leads to electronic sputtering.

The removal rate of surface atoms due to ion bombardment is quantified by the sputtering yield, Y, which is defined as the average number of atoms removed from the surface per incident ion [5]:

$$Y = \frac{average\ number\ of\ atoms\ removed}{number\ of\ incident\ ions} \tag{1}$$

The definition of sputtering yield implies that the average number of atoms removed is proportional to the number of incident ions. The sputtering yield is strongly dependent on the energy of the incident ions, the masses of the ions and target atoms, the experimental geometrical conditions (e.g., ion incidence angle) and the binding energy of atoms in the solid.

2. Experimental Method

Ion beam induced sputtering yield measurements were performed using the Time of Flight (ToF-ERDA) set up located on the zero-degree line of the 6 MV Tandem accelerator at iThemba LABS-TAMS, Gauteng. The ToF-Energy spectrometer, shown in the schematic in Figure 1, detects atoms forward recoiled from the target sample by the incident beam. Coincident measurement of the ToF and Energy allows for recoil atoms to be separated according to atomic mass, and so it then becomes possible to determine elemental spectra, from which depth profiles can be calculated [6].
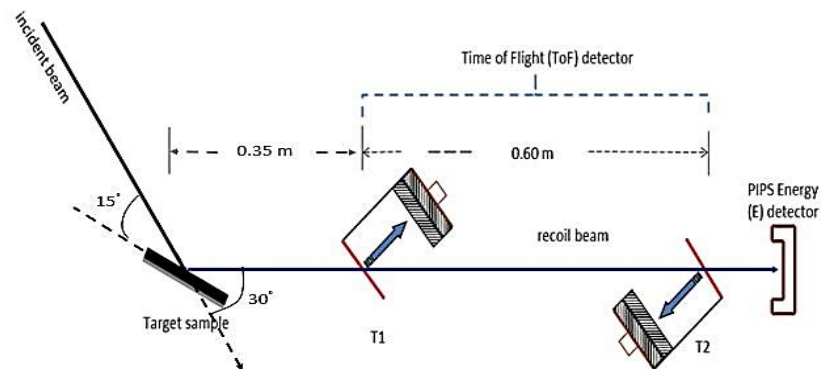

Figure 1. A schematic representation of the ToF-ERDA telescope configuration at iThemba LABS-TAMS [7].

Indium Tin Oxide (ITO)-on-glass samples of thickness ~32 nm (or ~253×10^15 atoms/cm²) were used in the irradiation measurements. The samples were mounted on a stainless-steel ladder located at the

center of a target chamber. The pressure in the chamber was maintained at 2×10^{-6} mbar during the measurements. The targets were placed at a tilted grazing incidence angle of 15º, with respect to the beam. The samples were uniformly irradiated for different irradiation times using three sets of energies for the Au^{q+} (20, 30 and 40 MeV) and Cu^{q+} (18, 27 and 34 MeV) collimated beams. The acceleration voltage, obtainable beam current for different charge states and the desired incident ion energy determines the ion charge state that eventually comes through to the experimental station. The ToF-Energy detector telescope used for the detection and identification of recoil ions is set at a forward scattering angle of 30º to the initial beam direction [8]. Measurements were carried out at an existing installation of the ERDA technique set up at iThemba LABS TAMS, where the ToF detector is at a fixed angle of 30º. The original choice of 30º was based on kinematic considerations to prevent flooding of the detector by forward scattered incident ions during routine Heavy Ion ERD thin film analysis [7].

A two-dimensional spectrum of ToF versus Energy was generated for the different incident ion energies used. The spectra gave well separated bands of the different elements present in the films, as shown in Figure 2. The spectra were analyzed to obtain depth profile information using a Heavy Ion ERDA software called Potku [9].
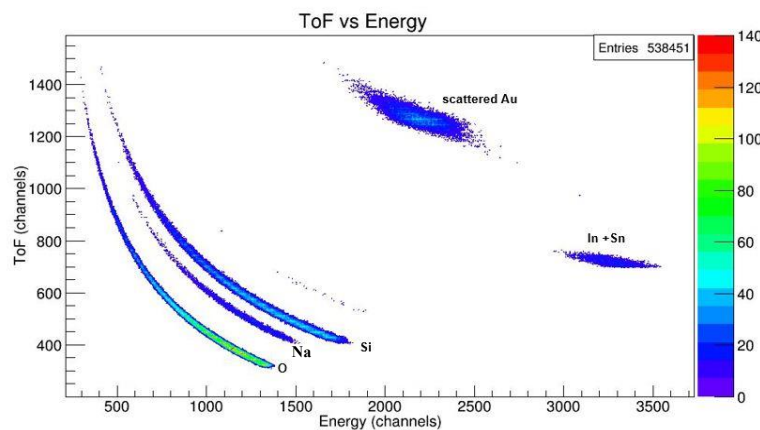
Figure 2. ToF-Energy scatter plot of an ITO film-coated glass substrate measured using a 40 MeV Au^{8+} incidence beam.

The beam fluence ϕ was calculated from the irradiation time t, beam current I and the beam spot area A on the target [8]:

$$\phi = \frac{It}{qeA} \tag{2}$$

where q is the ionic charge and e is the electron charge (1.602×10^{-19} C). The reduction in the thickness of the films due to sputtering was determined in terms of areal concentration from the Potku calculated depth profiles and the sputtering yield rate was determined from the slope of a graph of film thickness versus beam fluence.

The pristine and irradiated thin films were also subjected to Ultraviolet Visible measurements (LAMBDA 365 PerkinElmer Spectrophotometer) to investigate the changes in the optical band gap.

3. Results and Discussion

3.1. Sputtering Yields of ITO/Glass
For beam induced sputtering yield measurements, the irradiation fluence was extended beyond normal ERDA analysis measurement times to obtain a measurable decrease in the thickness of the ITO film.

Figure 3 depicts the change in atomic concentration of ITO as fluence is varied, as measured with a 30 MeV Au[7+] ion beam. As the beam fluence increases, the atomic concentration of oxygen decreases, as a result of oxygen atoms being sputtered from the ITO film. A similar comparison for atomic concentrations of indium and tin (In + Sn) shows fairly constant concentrations with increasing beam fluence, this is interpreted as an indication of insignificant sputtering of the In + Sn atomic species. The above-observed results of the relative decrease in O concentrations and constant In + Sn concentrations with increasing fluence, indicates a case of preferential sputtering; whereby oxygen atoms are sputtered at a higher rate than either In or Sn atoms.
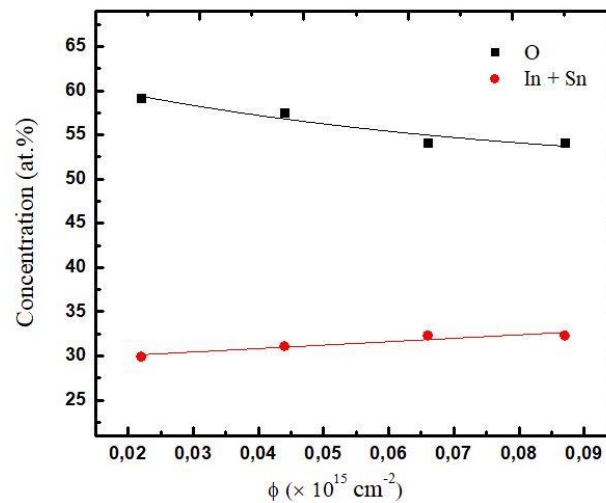

Figure 3. Concentrations of O and In + Sn in the ITO/glass thin film at different sputtering fluences measured using a 30 MeV Au[7+] ion beam.

Figures 4 and 5 shows plots of sputtering yields of oxygen as a function of incident Au and Cu ion beam fluence, respectively. The sputtering yield was obtained from the change in areal concentration against the ion fluence i.e., dividing the content of an element at two points in the initial part of the plot by the corresponding fluence values. The sputtering yield of oxygen by incident Au and Cu ions decreases with increasing ion fluence for the measured fluence range, as shown in both figures. Similar behaviour of a decrease in the sputtering yield with an increase in bombarding fluence was recently reported by Mammeri *et al*. [10], in the case of Bismuth thin films irradiated by swift Cu^{q+} heavy ions over the 10 to 26 MeV range and ion beam fluences of approximately $10^{13} - 10^{15}$ ions/cm². The decrease in the sputtering yields with increasing ion fluence can be attributed to the inelastic collisions causing changes in the ITO film thickness under heavy ion irradiation, due to large deposited electronic energy density.

Two different trends are also observed for sputtering yields versus beam fluence, obtained by the different Au and Cu beams as shown in Figures 4 and 5; for Au beam irradiations it can be noted that the sputtering yield rate shows a steep drop at low fluences and then tends to flatten as the fluence increases and for Cu beam irradiations the sputtering yield rate decreases gradually at first and then shows a steep drop as the fluence increases. Comparing the sputtering yields obtained by both Au and Cu beams, it can be noted that the sputtering yields for Au ions are larger than that of Cu ions. This can be explained in terms of the velocity effect based on the inelastic thermal spike model [11], which states that the relationship between the electronic sputtering yield is directly proportional to the area of the ion damage zone. The velocities of the Au ions are approximately 2.6 times smaller than that of Cu ions, thus lower velocity ions deposit high energy density resulting in a high ion damaged zone and higher sputtering yields.
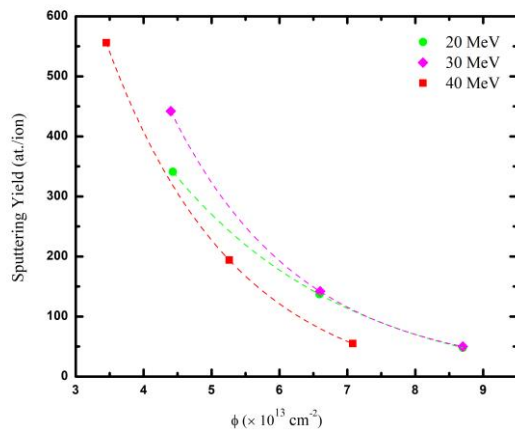
Figure 4. Sputtering yields versus ion fluence of O atoms from ITO/Glass thin films irradiated by 20, 30 and 40 MeV Au^{q+} ions.
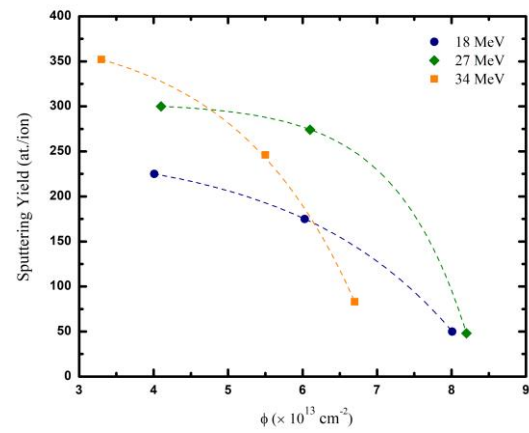

Figure 5. Sputtering yields versus ion fluence of O atoms from ITO/Glass thin films irradiated by 18, 27 and 34 MeV Cu^{q+} ions.

3.2. Secondary Irradiation Effects

Ultraviolet-Visible Spectroscopy (UV-Vis) was used to study the secondary irradiation effects of ITO thin films in comparison to unirradiated ITO thin films. Figures 6 and 7 shows the plots of $(\alpha h\nu)^2$ versus $(h\nu)$ for Au and Cu ion irradiated films, respectively. The value of the optical band gap is obtained by a method of extrapolating (Tauc's extrapolation) the linear part of the plot which intersects the x-axis at zero absorption, this gives the energy band gap. A slight decrease in the energy band gap of the Au and Cu irradiated films is seen from Figures 6 and 7. The energy band gap of the ITO thin films irradiated by 40 MeV Au^{8+} ions was slightly reduced from a pristine band gap value of 3.99 eV to 3.93 eV and those irradiated by 34 MeV Cu^{7+} ions slightly reduced from 3.99 eV to 3.95 eV with increases in ion fluences, this was concluded to be an insignificant reduction in the band gaps.
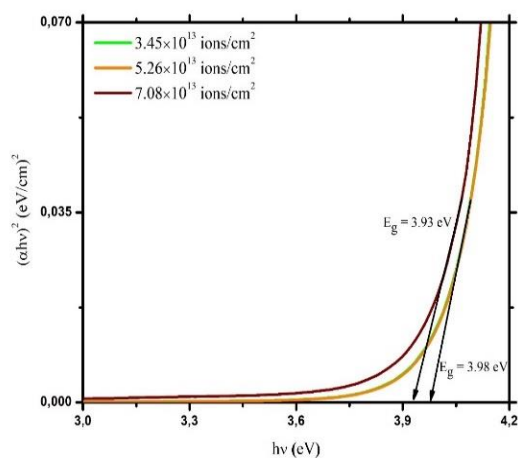
Figure 6. Plot of $(\alpha h\nu)^2$ versus Photon energy $(h\nu)$ for 40 MeV Au^{8+} ion irradiated ITO films coated glass substrate.
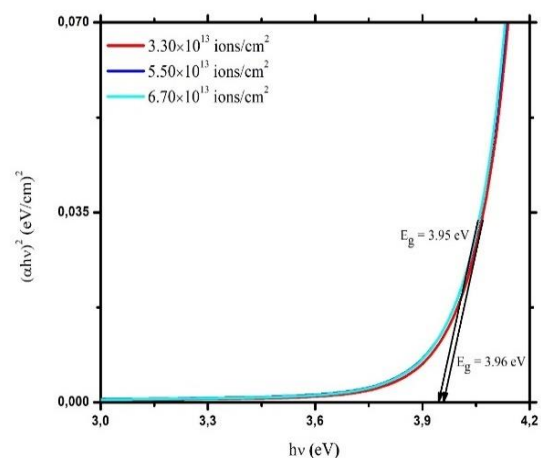
Figure 7. Plot of $(\alpha h\nu)^2$ versus Photon energy $(h\nu)$ for 34 MeV Cu^{7+} ion irradiated ITO films coated glass substrate.

4. Conclusion

Sputtering and secondary irradiation effects studies on ITO thin films were carried out. The reduction in thicknesses of the ITO films was attributed to the preferential sputtering of oxygen from the surface, as a consequence of weakly bonded oxygen atoms in the crystal lattice of the film. Electronic sputtering yields decrease with increasing ion fluences for both Au and Cu ion beams. The sputtering yields were found to be in the range of $10^1 - 10^2$ atoms/ion. The observed oxygen sputtering yields from the ITO thin films irradiated by Au ions were higher as compared to those irradiated by Cu ions. An insignificant decrease in the optical band gap as a function of ion fluence confirms that no changes in the optical properties occurred.

5. Acknowledgments

References

[1] Arnoldbik W M, Tomozeiu N and Habraken F H P M 2003 *Nucl. Instruments Methods Phys. Res. Sect. B Beam Interact. with Mater. Atoms*. **203** 151–157

[2] Madito M J, Terblans J J, Swart H C and Mtshali C B 2020 *South African J. Sci. Technol*. **39** 40–45

[3] Sigmund P 2012 *Nanofabrocation by Ion-Beam Sputtering: Fundamentals and applications* (Singapore: Pan Stanford Publishing) pp 1–40

[4] Fearn S 2015 *An Introduction to Time-of-Flight Secondary Ion Mass Spectrometry (TOF-SIMS) and its Applications to Materials Science* (USA: Morgan & Claypool) pp 1-6

[5] Sigmund P 1969 *Phys. Rev*. **184** 383–416

[6] Nastasi M, Mayer J W and Wang Y 2014 *Ion Beam Analysis Fundamentals and Applications* (New York: CRC Press) pp 79–100

[7] Msimanga M 2010 PhD Thesis University of Cape Town

[8] Mavhungu H, Msimanga M and Hlatshwayo T 2015 *Nucl. Instruments Methods Phys. Res. Sect. B Beam Interact. with Mater. Atoms*. **349** 79–84

[9] Arstila K *et al*. 2014 *Nucl. Instruments Methods Phys. Res. Sect. B Beam Interact. with Mater. Atoms*. **331** 34–41

[10] Mammeri S, Msimanga M, Dib A, Ammi H and Pineda-Vargas C A 2018 *Surf. Interface Anal*. **50** 328–334

[11] Wang Z G, Dufour C, Cabeau B, Dural J, Fuchs G, Paumier E, Pawlak F and Toulemonde M 1996 *Nucl. Instruments Methods Phys. Res. Sect. B Beam Interact. with Mater. Atoms*. **107** 175–180